

# Enhancing Solubility of Anthrarufin by Tethering Alkyl Phosphonate and Mitigating Capacity Decay with Additive in Aqueous Organic Redox Flow Batteries

Richa Gupta<sup>1</sup>, Chinmaya Mirlle<sup>1</sup>, Kothandaraman Ramanujam<sup>1\*</sup>

<sup>1</sup>*Clean Energy Laboratory, Department of Chemistry, Indian Institute of Technology Madras, Chennai,  
Tamil Nadu, 600036, India*

\*Corresponding author's e-mail: rkraman@iitm.ac.in

## Supporting information

### S1. Synthesis of 1,5-diphosphorylated anthraquinone:

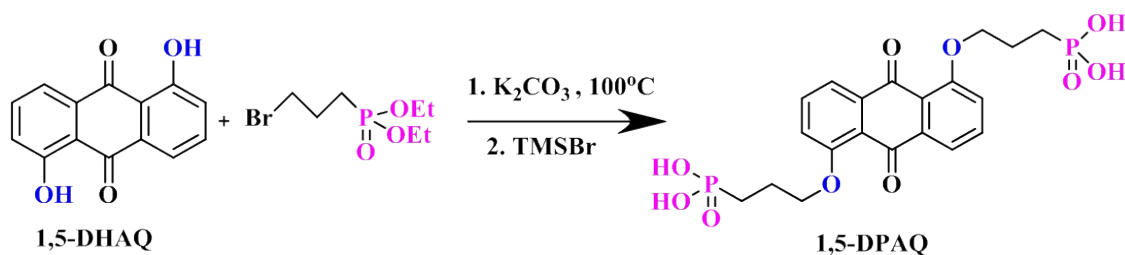
(((9,10-dioxo-9,10-dihydroanthracene-1,5-diyl)bis(oxy))bis(propane-3,1-diyl))bis(phosphonic acid) or 1,5-DPAQ has been synthesized using the modified procedure used in the literature.<sup>1</sup> Preparation of 1,5-DPAQ was done via a two-step synthesis process-

*Synthesis of ester precursor of 1,5-DPAQ: Tetraethyl (((9,10-dioxo-9,10-dihydroanthracene-1,5-diyl)bis(oxy))bis(propane-3,1-diyl))bis(phosphonate)*

30 mmol of diethyl (3-bromopropyl)phosphonate was added to the mixture of anhydrous K<sub>2</sub>CO<sub>3</sub> (40 mmol) in the 30 mL of DMF. 10 mmol of 1,5-DHAQ was then added to the reaction mixture and heated at 100°C overnight. Then, the mixture was kept for vacuum distillation to remove the solvent. The obtained solid was washed with distilled water and tested using the TLC method. The product was used for the next reaction step without further purification.

*Synthesis of 1,5-DPAQ: (((9,10-dioxo-9,10-dihydroanthracene-1,5-diyl)bis(oxy))bis(propane-3,1-diyl))bis(phosphonic acid)*

At the very next, the ester precursor of 1,5-DPAQ was dissolved in 60 mL of dichloromethane (DCM), and then trimethylsilyl bromide of 100 mmol was added. The reaction mixture was kept at room temperature for 18 h stirring. After stirring, the excess solvent was removed through distillation, and then the mixture was washed thoroughly with distilled water and hexane. A green solid was obtained after vacuum drying. Yield: 85%.  $^1\text{H NMR}$  (400 MHz,  $\text{DMSO-d}_6$ ):  $\delta = 7.77$  (2H, m), 7.70 (2H, d), 7.46 (2H, d), 4.196 (4H, t), 1.98 (4H, m), 1.84 (4H, m).



**Scheme S1.** Synthesis of 1,5-DPAQ.

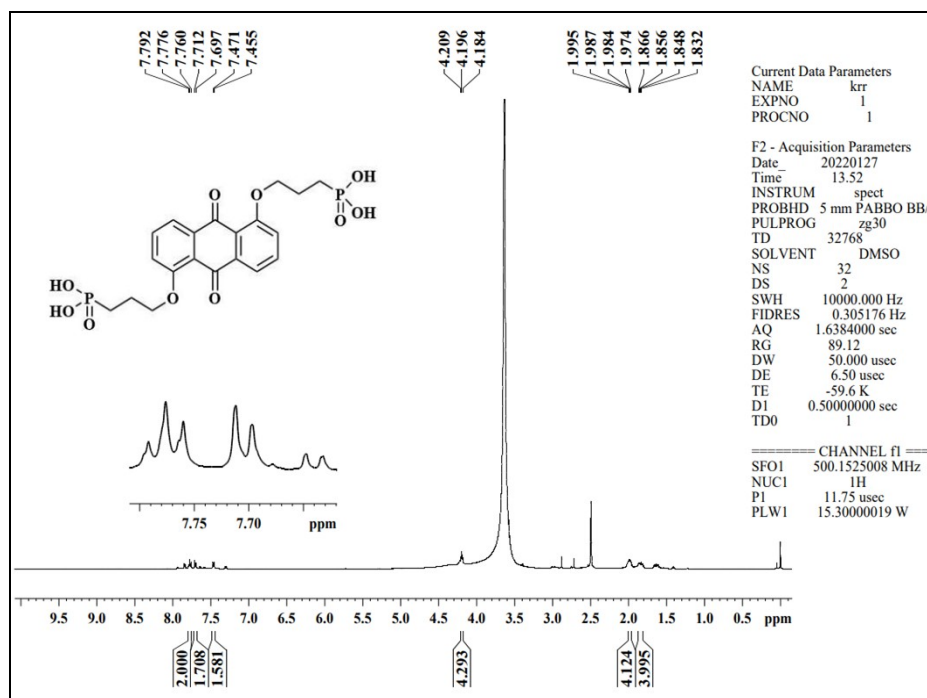


Fig. S1.  $^1\text{H-NMR}$  of 1,5-DPAQ in  $\text{DMSO-d}_6$ .

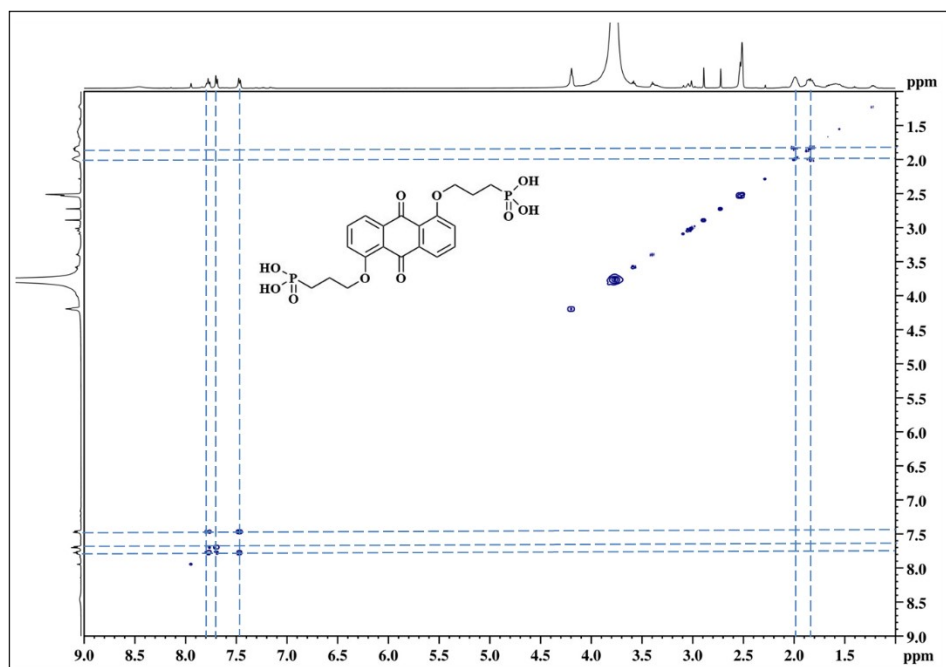


Fig. S2. COSY  $^1\text{H-NMR}$  of 1,5-DPAQ in  $\text{DMSO-d}_6$ .

## **S2. Solubility tests:**

KOH electrolytes with different pHs of 14, 12, and 9 were prepared to test the solubility of 1,5-DHAQ and 1,5-DPAQ in aqueous alkaline media. In order to test the solubility, precisely 20 mg of the sample has been taken in a test tube, followed by adding 10  $\mu$ L of electrolyte in an incremental period. An electrolyte was added until a clear solution was visually observed. After each addition, the test tube was shaken mechanically, and then the solution was heated at 50  $^{\circ}$ C, followed by cooling it down to room temperature. An average volume of electrolytes was used to estimate solubility just before and after the complete dissolution of samples. The solution has been kept for 24 hours to watch for precipitation, if any.

## **S3. Membrane and electrode activation:**

The 6 cm  $\times$  6 cm Nafion-117<sup>TM</sup> membrane was washed using 4% (w/v) H<sub>2</sub>O<sub>2</sub> for 30 min at 80  $^{\circ}$ C followed by washing with millipore water, then heated in 1 M H<sub>2</sub>SO<sub>4</sub> at 80 $^{\circ}$ C for 30 min and then washed off with millipore water to get rid of organic and inorganic containments, respectively. Before being utilized in the cell, the treated or activated membrane was soaked in 1 M KOH for 24 h. Carbon felt activation is required to increase the wettability of the electrode for usage in aqueous solutions. As a result, the carbon felt was pre-heated at 400  $^{\circ}$ C in the air for 24 h in a Sigma muffle furnace, where the hydrophilicity of the electrode was improved after the generation of carbonyl functional groups. This activated carbon felt (TGF) has been used during cell fabrication.

#### S4. Cell fabrication:

The acrylic end plates of 10 mm thickness, copper plates of 2 mm thickness as a current collector, and a 15 mm thick carbon block of area of 5 cm × 5.5 cm, with serpentine flow field of channel dimensions of 1.5 mm depth and 1.5 mm width, including land width of 1 mm were the cell components used. To prevent electrical contact between the anode and cathode, separator Nafion 117 was sandwiched between both electrodes. During cell fabrication, a 0.6 mm thick rubber gasket was placed around the carbon block to avoid any leakage. 5 cm × 5.5 cm TGF electrodes were placed on the carbon block's carved compartment to allow the electrolyte flow across the electrodes. Nearly 16% compression was achieved when the cell was assembled using nuts and bolts. The inlet and outlet at the end plates were connected via Teflons to the solution tanks through 4 mm silicon tubing. The flow rate of electrolytes was maintained at 25 mL min<sup>-1</sup> and circulated using a Ravel peristaltic pump (model RH-P100S-200-2H) throughout the cell. Throughout the cell's operation, argon gas was purged using a balloon introduced into the anolyte tank to maintain the inert atmosphere. These can be easily understandable via a picture of the fabricated cell (**Fig. S3**).

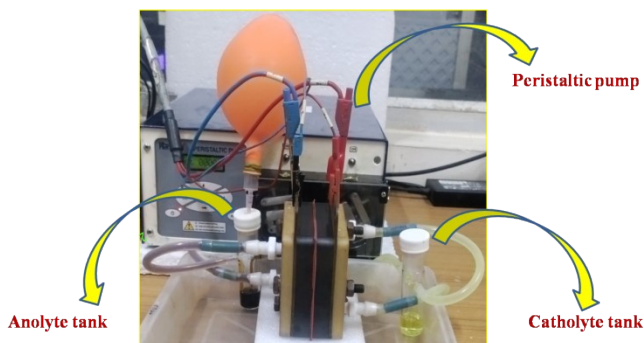


**Fig. S3.** Cell showing anolyte and catholyte flow through the electrode via a peristaltic pump. Argon balloon was inserted into the anolyte tank to maintain an inert atmosphere during cell cycling.

## S5. Electrochemical materials and characterizations:

Cyclic voltammetry (CV) and linear sweep voltammetry (LSV) were carried out using PGSTAT204-Metrohm multi-Autolab (MAC90009) Potentiostat/ Galvanostat. Glassy carbon electrodes (GCE) with a 7.07 mm<sup>2</sup> area were purchased from CH Instruments, Inc. and used as working electrodes (WE) for three electrode mode studies. Pt wire and Ag/AgCl (saturated KCl) were used as a counter electrode (CE) and reference electrode (RE) to carry out CV via three electrode modes. All the CV plots have been plotted after IR corrections via impedance recorded in each CV set-up. The Randles-Sevcik equation **S(1)** was used to determine the diffusion coefficient value ( $D$ , cm<sup>2</sup> s<sup>-1</sup>) of the redox species as;

$$i_p = 0.4463 n F S C \left( \frac{n F D \nu}{R T} \right)^{1/2} \quad \mathbf{S(1)}$$

where,  $i_p$  is the peak current for a given scan rate in A,  $n$  is the number of electrons involved during redox reactions,  $F$  is Faraday constant in C mol<sup>-1</sup>,  $S$  is the area of the GCE in cm<sup>2</sup>,  $C$  is the concentration in mol cm<sup>-3</sup>,  $\nu$  is scan rate in V s<sup>-1</sup>,  $R$ , and  $T$  is gas constant in J K<sup>-1</sup> mol<sup>-1</sup> and absolute temperature in K, respectively.

Nicholson method is used to estimate heterogeneous electron transfer rate ( $k^o$ ) in cm s<sup>-1</sup> by keeping the calculated  $D$  value (from the Randles-Sevcik eq.) in the given expression **S(2)**;

$$\Psi = k^o \left( \frac{\pi D n F}{R T} \right)^{-1/2} \nu^{-1/2} \quad \mathbf{S(2)}$$

Here,  $\Psi$  value is obtained from Klingler-Kochi equation **S(3)** as;

$$\Psi = \frac{(-0.6288 + 0.0021 \Delta E_p)}{(1 - 0.017 \Delta E_p)} \quad \mathbf{S(3)}$$

where  $\Delta E_p$  is the peak-to-peak separation between anodic and cathodic peak potential, and the rest have their usual meanings. To cross-identify the  $D$ ,  $\text{cm}^2 \text{s}^{-1}$  value, LSV was performed in three electrode mode using GCE ( $0.196 \text{ cm}^2$  area) as a working electrode purchased from Pine Research Instruments. The Levich equation **S(4)** was used to determine  $D$ ,  $\text{cm}^2 \text{s}^{-1}$  via LSV studies of the redox species as;

$$i_l = 0.201 n F S D^{2/3} \omega^{1/2} \mu^{-1/6} C \quad \mathbf{S(4)}$$

where,  $i_l$  is limiting current in A,  $\omega$  is rotations per minute,  $\mu$  is kinematic viscosity ( $1.07 \times 10^{-2} \text{ cm}^2 \text{s}^{-1}$ ) of 1 M KOH,<sup>2</sup> and rest have their usual meanings.

The galvanostatic charge-discharge (GCD) and electrochemical impedance spectroscopy (EIS) were recorded by using OrigaFlex (Orignalys) potentiostat. The crossover or degradation of the molecules was monitored through CV, NMR, and UV-Vis studies. NMR and UV-Vis have been recorded with Bruker NMR and SHIMADZU UV-VIS spectrophotometer (UV-1780), respectively, as well as a CV to monitor crossover or degradation studies.

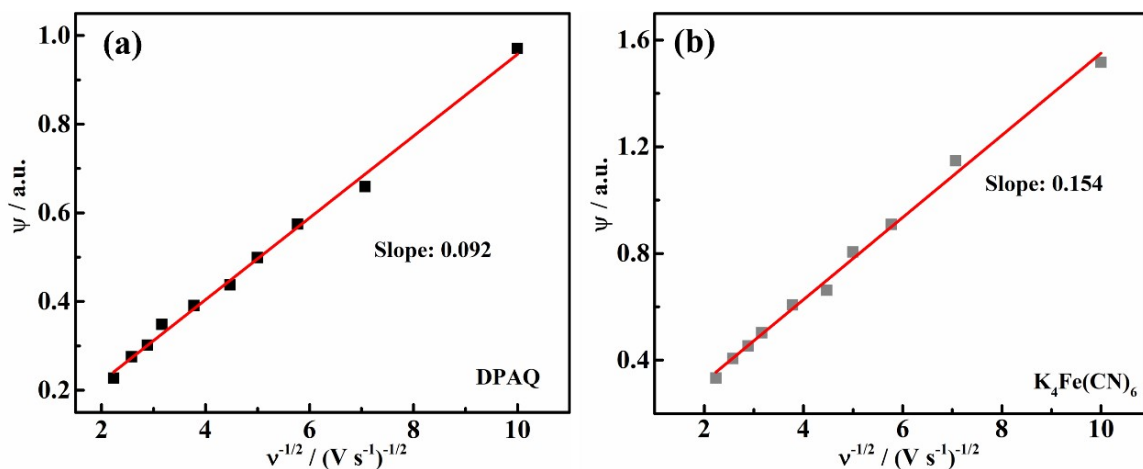


**Fig. S4.** Linear relationship plot of  $\phi$  vs.  $\nu^{1/2}$  of 5 mM of (a) 1,5-DPAQ and (b)  $\text{K}_4[\text{Fe}(\text{CN})_6]$  in 1 M KOH at a scan rate of  $50 \text{ mV s}^{-1}$  using GCE as working electrodes, Ag/AgCl as a reference and Pt wire as a counter electrode.

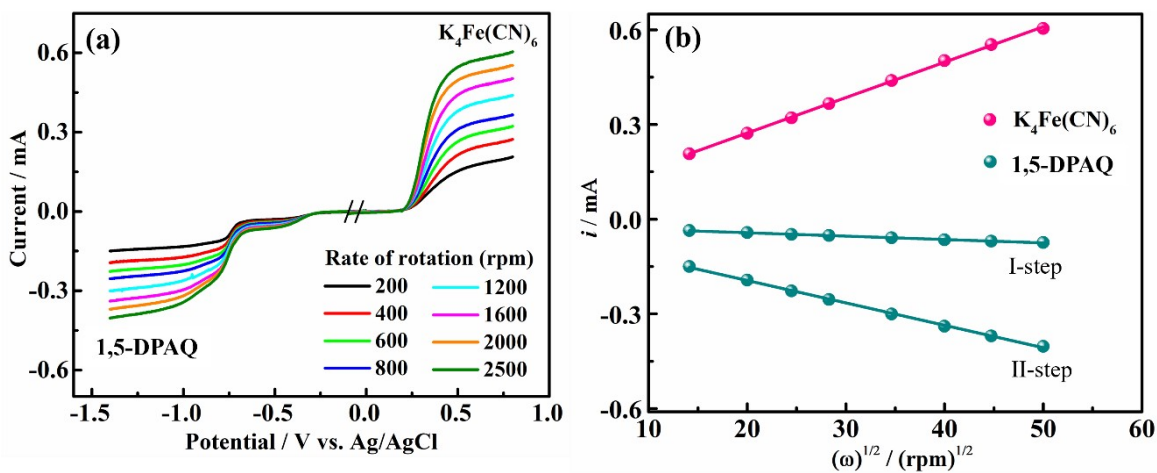


**Fig. S5.** (a) LSV plot and (b)  $i_l$  vs.  $\omega^{1/2}$  plot for 7 mL of 5 mM 1,5-DPAQ and  $\text{K}_4[\text{Fe}(\text{CN})_6]$  in 1 M KOH.

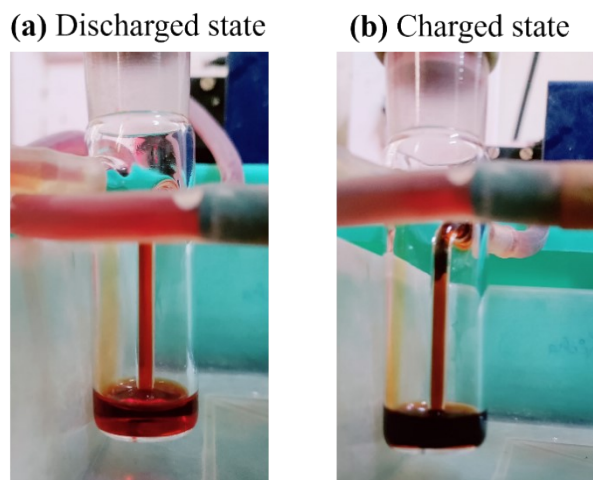


**Fig. S6.** Photographic image of colour change with change in oxidation state of 1,5-DPAQ at (a) discharged (light brown-red) and (b) charged (dark brown-red) states.

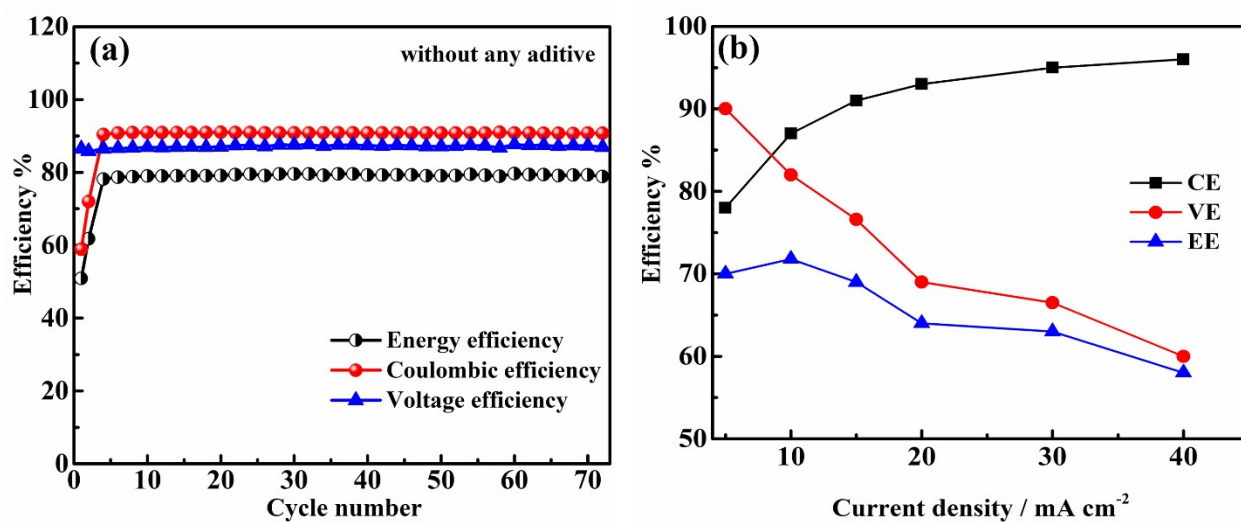


**Fig. S7.** (a) Efficiency plot at 10 mA cm<sup>-2</sup> current density for initial 74 cycles. (b) The trend of efficiencies with respect to the increase in current densities.

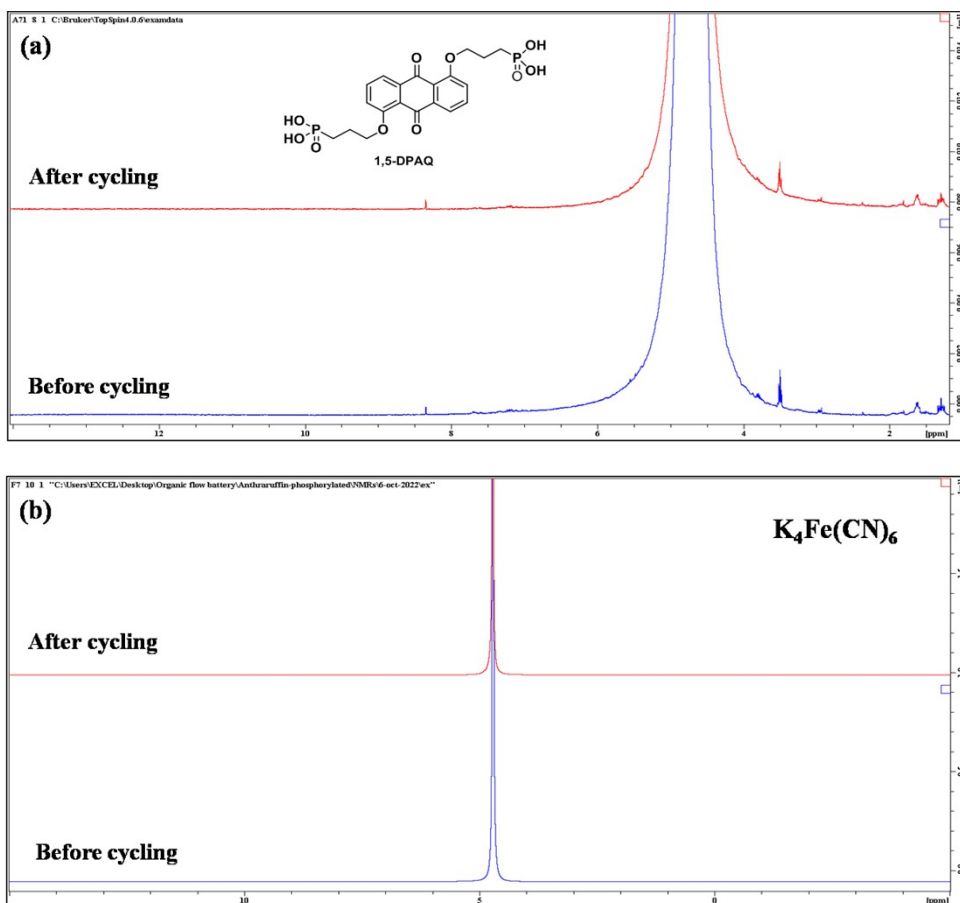


**Fig. S8.**  $^1\text{H-NMR}$  of (a) 1,5-DPAQ and (b)  $\text{K}_4[\text{Fe}(\text{CN})_6]$  before and after 50 cycles. The sample withdrawn was diluted suitably with  $\text{D}_2\text{O}$  solvent for NMR measurement.

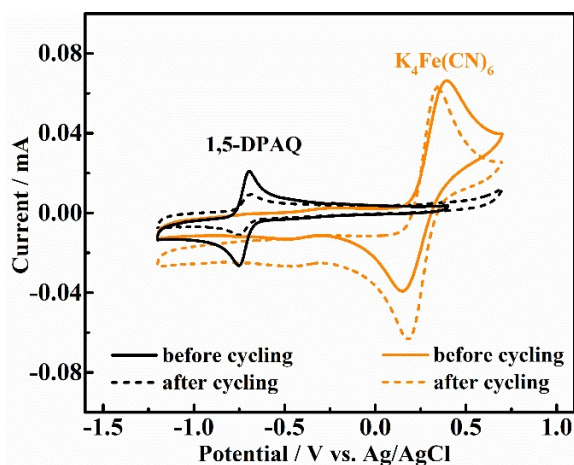


**Fig. S9.** CV of 1,5-DPAQ and  $\text{K}_4[\text{Fe}(\text{CN})_6]$  before and after cycling for 50 cycles using Nafion-117 as a separator, using GCE as working electrodes,  $\text{Ag}/\text{AgCl}$  as a reference and Pt wire as a counter electrode.

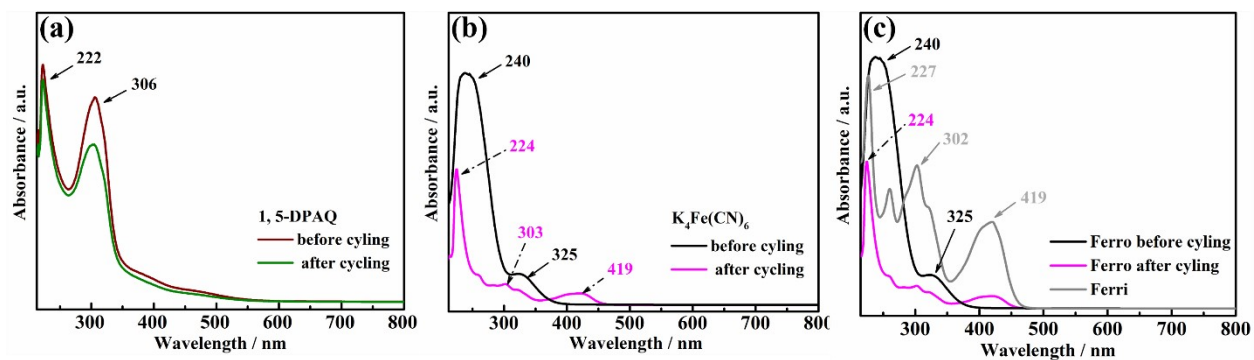


**Fig. S10.** UV-vis study before and after cycling for 50 cycles (a) 1,5-DPAQ and (b)  $K_4[Fe(CN)_6]$  and comparative plot of (c)  $K_3[Fe(CN)_6]$  with  $K_4[Fe(CN)_6]$ .

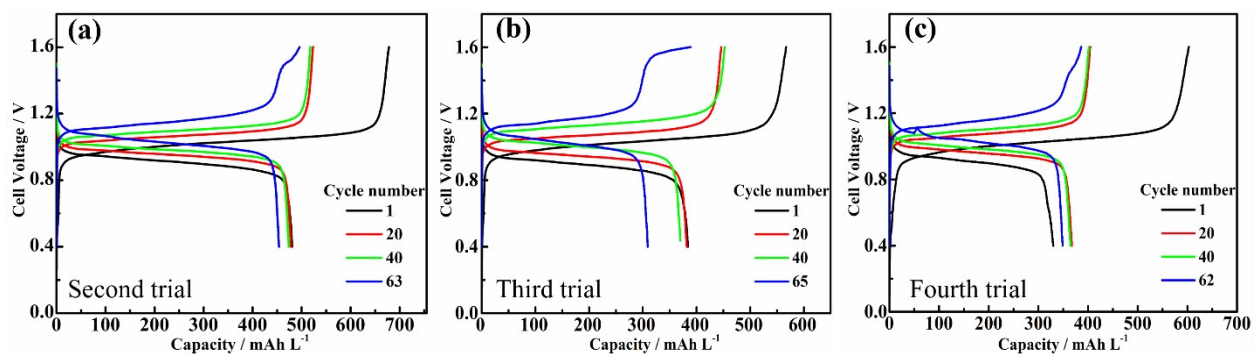


**Fig. S11.** Galvanostatic charge-discharge of 20 mL of 20 mM 1,5-DPAQ || 100 mM  $K_4[Fe(CN)_6]$  showing an appearance of the extra plateau at 1.4 V during the charging of the cell in (a) second, (b) third, and (c) fourth trials.

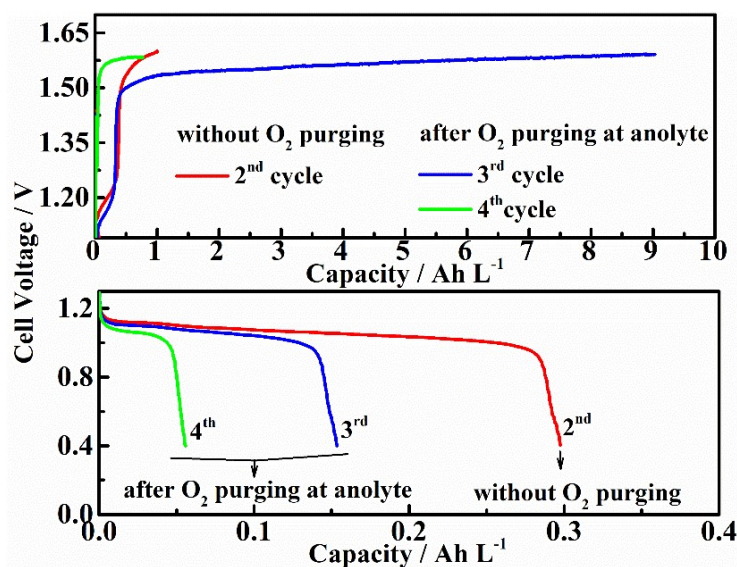


**Fig. S12.** Galvanostatic charge-discharge data showing charge curves (top tile) and discharge curves (bottom tile) of cell 20 mM 1,5-DPAQ || 100 mM K<sub>4</sub>[Fe(CN)<sub>6</sub>] in 20 mL of 3 M KOH with and without oxygen purging at the anolyte

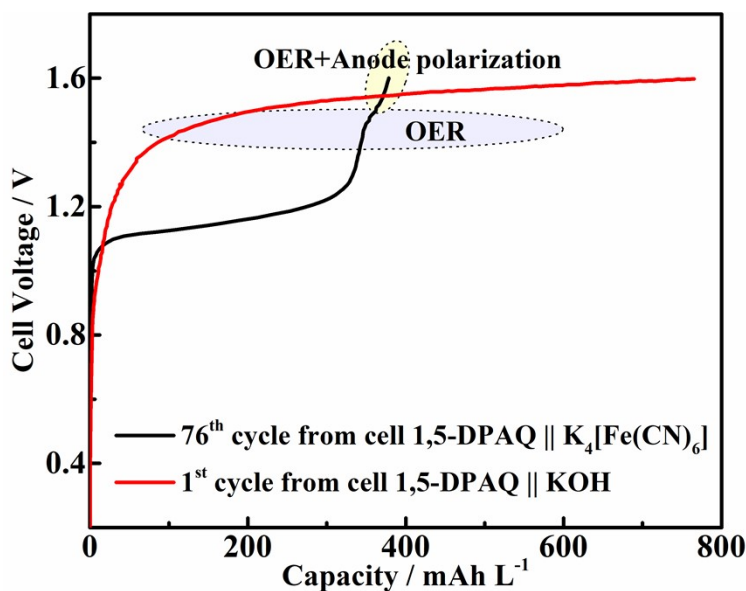


**Fig. S13.** Comparative plot of galvanostatic charging of cell 20 mM 1,5-DPAQ || 100 mM K<sub>4</sub>[Fe(CN)<sub>6</sub>] (black line) and 20 mM 1,5-DPAQ || 1M KOH (red line) at 10 mA cm<sup>-2</sup> highlighting OER and OER+anode polarization region.

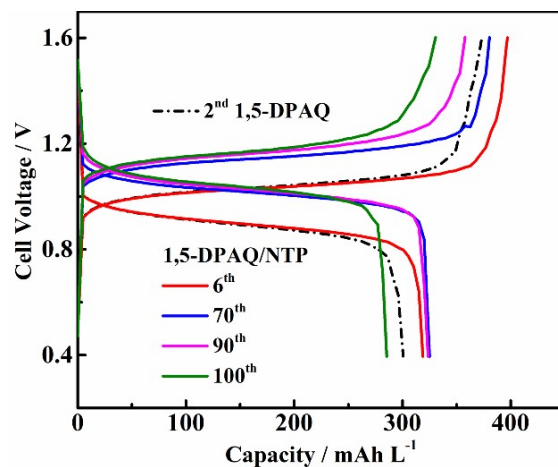


**Fig. S14.** Galvanostatic charge-discharge plot of 17 mL, 20 mM 1,5-DPAQ/(3 mL) NTP || 20 mL, 100 mM  $K_4[Fe(CN)_6]$  in 1 M KOH recorded at  $10 \text{ mA cm}^{-2}$  (where NTP was present from 5<sup>th</sup> cycle).

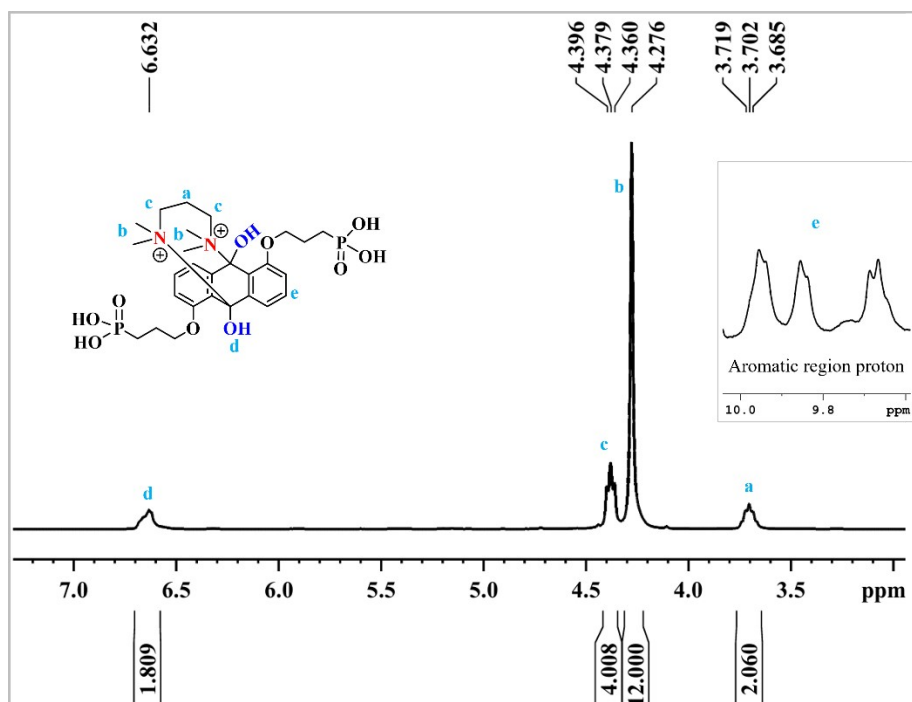
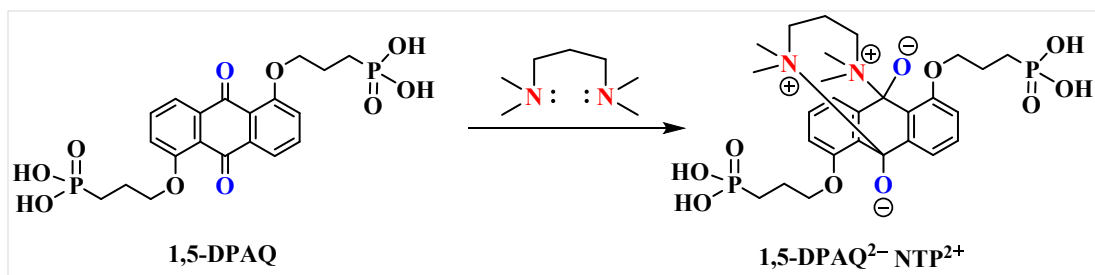


**Fig. S15.**  $^1\text{H-NMR}$  of 1,5-DPAQ added NTP using a mixture of  $\text{DMSO-d}_6$  and  $\text{D}_2\text{O}$  solvent recorded with reference to  $\text{D}_2\text{O}$  solvent (thus peak shifted) (note: the NTP's peak is highly intense due to comparatively 53 times higher molar ratio used than that of 1,5-DPAQ).



**Scheme S2.** Interaction of 1,5-DPAQ with NTP.

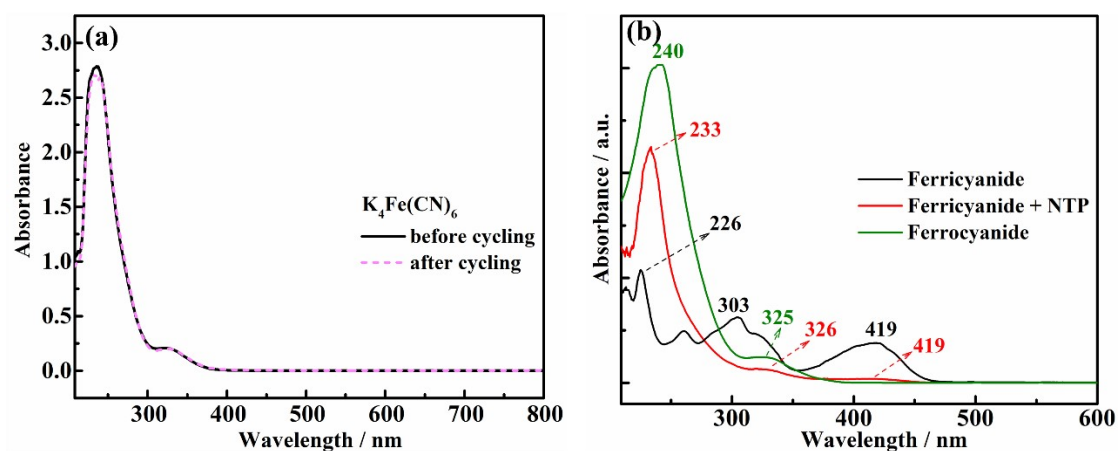


**Fig. S16.** Post-cycling UV-Vis studies of (a)  $\text{K}_4[\text{Fe}(\text{CN})_6]$  before and after 100 cycles and (b) ferricyanide and its mixture with NTP and ferrocyanide solution.

## References

- 1 Y. Ji, M. Goulet, D. A. Pollack, D. G. Kwabi, S. Jin, D. De Porcellinis, E. F. Kerr, R. G. Gordon and M. J. Aziz, *Adv. Energy Mater.*, 2019, **9**, 1900039.
- 2 A. S. Lileev, D. V Loginova and A. K. Lyashchenko, *Russ. J. Inorg. Chem.*, 2011, **56**, 961–967.